Simulated Global-Mean Sea Level Changes over the Last Half-Millennium

J. M. GREGORY

Department of Meteorology, University of Reading, Reading, and Hadley Centre, Met Office, Exeter, United Kingdom

J. A. LOWE AND S. F. B. TETT

Hadley Centre, Met Office, Exeter, United Kingdom

ABSTRACT

Simulations of the last 500 yr carried out using the Third Hadley Centre Coupled Ocean–Atmosphere GCM (HadCM3) with anthropogenic and natural (solar and volcanic) forcings have been analyzed. Global-mean surface temperature change during the twentieth century is well reproduced. Simulated contributions to global-mean sea level rise during recent decades due to thermal expansion (the largest term) and to mass loss from glaciers and ice caps agree within uncertainties with observational estimates of these terms, but their sum falls short of the observed rate of sea level rise. This discrepancy has been discussed by previous authors; a completely satisfactory explanation of twentieth-century sea level rise is lacking. The model suggests that the apparent onset of sea level rise and glacier retreat during the first part of the nineteenth century was due to natural forcing. The rate of sea level rise was larger during the twentieth century than during the previous centuries because of anthropogenic forcing, but decreasing natural forcing during the second half of the twentieth century tended to offset the anthropogenic acceleration in the rate. Volcanic eruptions cause rapid falls in sea level, followed by recovery over several decades. The model shows substantially less decadal variability in sea level and its thermal expansion component than twentieth-century observations indicate, either because it does not generate sufficient ocean internal variability, or because the observational analyses overestimate the variability.

1. Introduction

Future sea level rise has the potential to cause loss of life and damage to man-made assets and natural habitats. To have confidence in projections for the future we must be able to account for observed past changes in sea level.

Global-mean sea level rise on decadal time scales is caused by warming and hence reduction in density of seawater, and by increase in the mass of the ocean through transfer of water from other stores in the climate system. According to the assessment of Church et al. (2001), thermal expansion provided the largest contribution to global-mean sea level rise during the twentieth century, with loss of mass by glaciers and ice caps giving approximately half as much. They also noted

Corresponding author address: J. M. Gregory, Department of Meteorology, University of Reading, P.O. Box 243, Reading RG6 6BB, United Kingdom.
E-mail: j.m.gregory@reading.ac.uk

that the uncertainty on each contribution was large and that their sum was somewhat smaller than the 1.0–2.0 mm yr^{-1} sea level rise estimated from tide gauges—an inconsistency that Munk (2002) called the "enigma" of sea level rise.

In this work we analyze multicentury climate model simulations of the past driven by natural and anthropogenic forcing and compare the contributions to global-mean sea level with observations. We address several questions that are relevant to understanding the observed record of global-mean sea level change and detecting anthropogenic influences:

- Can climate model simulations replicate observed multicentury sea level change?
- What is the relative importance of thermal expansion and the land ice terms in sea level change before and during the twentieth century?
- What is the relative importance of natural and anthropogenic forcing on sea level change?
- What size of variations in sea level occur in the absence of anthropogenic forcing?

TABLE 1. List of HadCM3 experiments analyzed in this work. The "Start" column shows the first year of the experiment. CONTROL runs in parallel to all the others and has nominal dates. All of the other experiments run to the end of the twentieth century. The "N" column indicates the number of experiments run as an ensemble with this forcing

Name	Start	N	Forcing
CONTROL	—	1	Constant late-nineteenth-century greenhouse gas concentrations, late-twentieth-century land surface properties and orbital configuration, average twentieth-century volcanic aerosol, solar irradiance of 1365 W m^{-2}.
NAT500	1492	1	Natural: volcanic aerosol, solar variability, and orbital changes. Constant well-mixed greenhouse gases and land surface properties for 1750.
ALL250	1750	1	Natural as in NAT500. Anthropogenic changes in greenhouse gases, anthropogenic sulfate aerosols, and land surface properties.
NAT	1860	4	Natural: the solar forcing increase from the nineteenth to the twentieth century was smaller than in NAT500, the forcing from the eruption of Krakatau in 1883 was more negative, and orbital changes were omitted.
ANTHRO	1860	4	Anthropogenic as for ALL250, except that land surface properties were constant; deforestation produces an increasingly negative forcing in ALL250.
ALL	1860	4	Natural as in NAT and anthropogenic as in ANTHRO.
VOL	1940	4	Volcanic as in NAT.
VOL5	1860	1	Volcanic as in NAT, multiplied by 5 to produce a clearer signal.

We begin by outlining the design of the climate model experiments. Next we describe the methods used to compute the thermal expansion and land ice contributions to sea level and compare the results with observational estimates of these terms. Finally we compare the simulated results for global-mean sea level change from the experiments with one another and with tide gauge and altimeter results in order to address the above questions.

2. Experimental design

Our simulations were carried out using the Third Hadley Centre Coupled Ocean–Atmosphere GCM (HadCM3), which is an unfluxadjusted atmosphere–ocean general circulation model (AOGCM) having a resolution of 2.5° latitude × 3.75° longitude × 19 levels in the atmosphere, and 1.25° × 1.25° × 20 levels in the ocean. More details of the model and its parameterizations and CONTROL experiment (with constant radiative forcing) are given by Gordon et al. (2000), Pope et al. (2000), and Collins et al. (2001). The experiments used in the current work are detailed in Table 1.

We concentrate on the new simulations NAT500 and ALL250 of Tett et al. (2006). NAT500 starts in 1492 with natural forcings only, and ALL250 starts in 1750 from the conditions of NAT500 for that year. In starting the NAT500 simulation from 1492 we imposed a step change in radiative forcing of -0.28 W m^{-2}, the difference between the initial forcing of NAT500 and the CONTROL forcing. In the analysis of results from NAT500 and ALL250 the effect of this step change was removed with the aid of linear Green's functions [a sum of two exponentials with different time scales, following Voss and Mikolajewicz (2001)] fitted to the response of

global-mean surface warming and thermal expansion (Fig. 1) to a rapidly imposed large CO_2 forcing, as simulated by a 1000-yr HadCM3 experiment.

Comparison of NAT500 and ALL250 with the NAT, ALL, and ANTHRO simulations beginning in 1860 (Stott et al. 2000; Tett et al. 2002) allows us to evaluate the "commitment" to sea level rise caused by forcing changes before this date. Since these experiments are ensembles of integrations starting from slightly different initial conditions, they also give information about the magnitude of internally generated variability. The comparison is hampered by the forcings not being exactly the same as in NAT500 and ALL250 (see Table 1), mainly because of updates made to the reconstruction of natural forcing from proxy evidence. Hegerl et al. (2003) estimate a 5%–95% confidence interval of ±50% for volcanic forcing and Ramaswamy et al. (2001) ±67% for solar forcing.

We use the VOL5 (Stott et al. 2003) and VOL integrations to isolate the effect of volcanic forcing.

3. Surface air temperature

During the twentieth century ALL250 shows a rise in global-mean surface air temperature change that is similar to the observational estimate from the Hadley Centre/Climate Research Unit of the University of East Anglia global surface air temperature dataset (HadCRUG; Folland et al. 2001). The fitted trends are 0.56 ± 0.13 and 0.64 ± 0.09 K century^{-1} for ALL250 and HadCRUG (Fig. 2). (These linear trends are intended only for an informal comparison. Their uncertainties come from the residuals of the least squares fit.) The time series have a similar form, with a period of warming in the first half of the century, a pause or weak cooling for
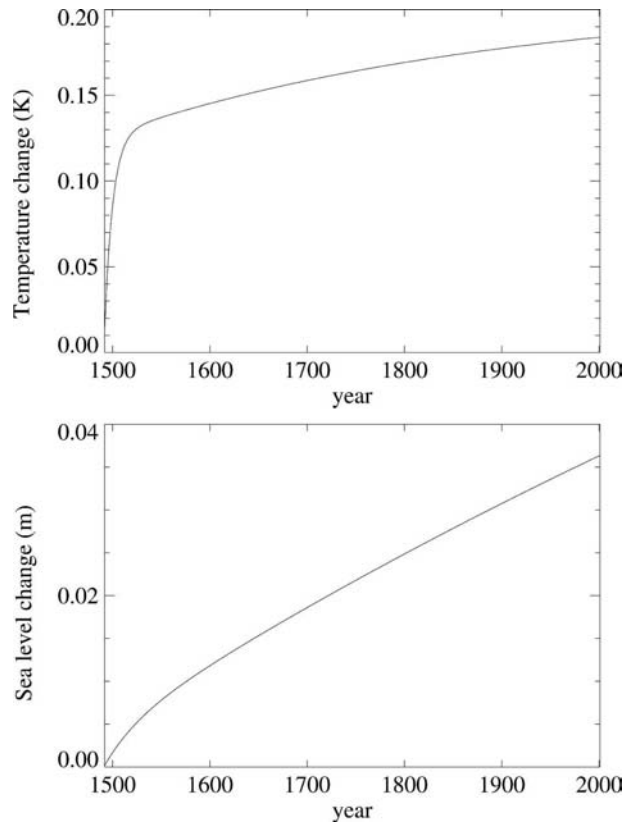
FIG. 1. Time series of the corrections to be added to global-mean SAT and sea level rise due to thermal expansion in order to remove the effect of the step change in forcing at the start of NAT500.
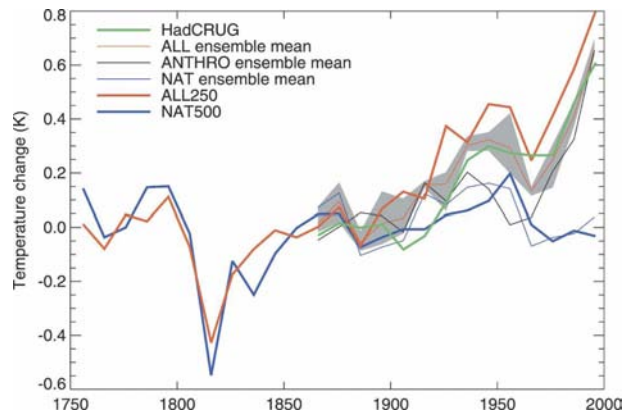

FIG. 2. Global-mean SAT change from the HadCRUG observational dataset (Folland et al. 2001), the HadCM3 ensemble simulations of Stott et al. (2000), and the ALL250 and NAT500 simulations of Tett et al. (2006). The time series have been shifted vertically so that each has a mean of zero for 1865–94. The gray shading shows the envelope of the four simulations of the ALL ensemble.

20–30 yr and a recent resumption of warming. A good reproduction of historical surface air temperature changes does not guarantee that simulated sea level changes will be realistic, for instance because it could depend on compensating errors in climate sensitivity and ocean heat uptake efficiency, in which case the sea level rise due to thermal expansion would be unrealistic (Gregory and Lowe 2000; Raper et al. 2002). However, it is a necessary condition, since the rate of thermal expansion and land ice change are both sensitive to global-mean temperature. In particular the large sea level rise during the last decade (discussed in section 5d) may be in part due to recent rapid warming, whose rate is satisfactorily matched by ALL250.

The twentieth-century trend of the ALL ensemble average is 0.44 ± 0.07 K century^{-1}. This is statistically consistent with ALL250, but it is possible that ALL250 warms up more during the late nineteenth and early twentieth century; by around 1920 it has emerged from the envelope of the ALL ensemble, and thereafter warms at a similar rate to the ALL ensemble average. The natural forcing is larger in ALL250 than ALL (sec-

tion 2; Table 1), but this is probably not the reason for the different response since NAT500 and NAT are similar. A more likely explanation is that it is a response to the forcing caused by anthropogenic greenhouse gas emissions before 1860. ALL omits the effect of this forcing because it begins from CONTROL, which is a steady state for late-nineteenth-century atmospheric composition. An uncompleted response to previous positive forcing changes is associated with a net downward radiative flux at the top of the atmosphere, that is, a heat uptake by the climate system. This flux is more positive in ALL250 than in NAT500 around 1860 (Tett et al. 2006, their Fig. 3); it is $+0.13$ W m^{-2} (relative to the CONTROL) for 1855–65 in ALL250.
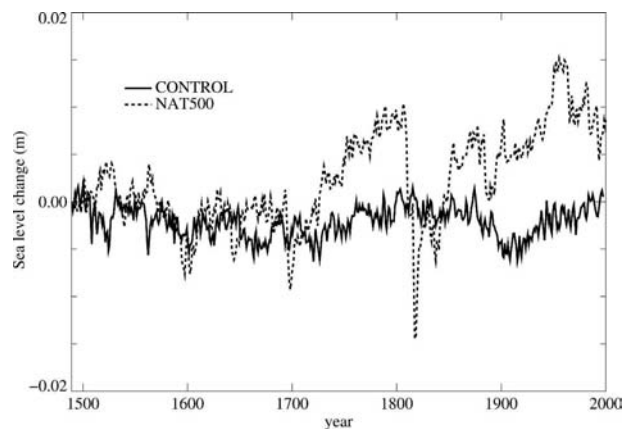

FIG. 3. Annual time series of global-mean sea level change due to thermal expansion in the HadCM3 CONTROL and NAT500 integrations. The time series have been shifted vertically to start from zero in 1492.

As found by Stott et al. (2000), anthropogenic forcing alone does not reproduce the observed temperature record. ANTHRO warms rapidly in recent decades but lacks the warming in the first half of the twentieth century, which was probably due partly to solar and volcanic forcing, and is shown in NAT and NAT500. These runs cool in the second half of the century, suggesting that natural forcing has offset some of the anthropogenic warming in recent decades.

4. Contributions to global-mean sea level

a. Thermal expansion

1) METHOD

The thermal expansion component of sea level change was computed using the United Nations Educational, Scientific and Cultural Organization (UNESCO) equation of state applied to simulated changes in in situ ocean temperature (Gregory and Lowe 2000). Two corrections were applied to the thermal expansion time series. First, the CONTROL experiment, with fixed forcing, was used to evaluate the drift due to cooling in the deep layers (the model was not spun up to a completely steady state before the CONTROL began); a cubic polynomial fit to this time series was then subtracted from the results of all the other integrations. Second, as mentioned in the experimental design, a correction was applied in NAT500 and ALL250 to account for the sea level response to the step in forcing at the start of NAT500 (Fig. 1).

Using the ALL250 results, we calculate that 1.7×10^{10} J m^{-2} of heat would need to be added to the ocean for each meter of thermal expansion, equivalent to an average thermal expansivity of 3.2×10^{-4} K^{-1}. Our value is similar to that of 2.0×10^{10} J m^{-2} found by Russell et al. (2000) for the Goddard Institute for Space Studies (GISS) AOGCM. Differences in this quantity reflect the distribution of simulated warming within the ocean, since thermal expansivity depends on temperature, pressure, and salinity. The values obtained by using the early and later parts of ALL250 separately were similar, suggesting that this distribution changes little during the experiment.

2) VARIABILITY OF SEA LEVEL DUE TO THERMAL EXPANSION

Natural external forcing (from solar variability and volcanic eruptions), which is in NAT500 but not in CONTROL, inflates the temporal variability of surface climate, and hence of ocean heat uptake and sea level change due to thermal expansion. The interannual
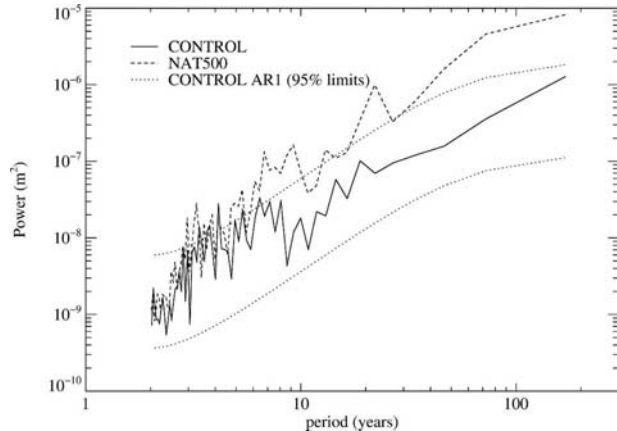

FIG. 4. Power spectra of variations in global-mean sea level due to thermal expansion in CONTROL and NAT500.

standard deviation of sea level over the 500 yr in CONTROL (Fig. 3) is 1.6 mm, while in NAT500 it is 3.5 times greater. The two time series exhibit a similar amplitude of high-frequency variations; however, NAT500 has some longer-period changes not seen in CONTROL. There is an apparent shift of regime during the eighteenth century, which makes the frequency distribution of thermal expansion for NAT500 bimodal, with one mode pre-1700, the other post-1800. The diagnosed forcings (Tett et al. 2006) suggest the increase in the modal value is likely to be due to a combination of increased solar forcing and reduced negative volcanic forcing during the eighteenth century.

The power spectra of NAT500 and CONTROL (Fig. 4) also show agreement at the highest frequencies but disagree at longer periods. NAT500 has considerably more power than CONTROL for periods of greater than 7 yr. A first-order autoregressive (AR1) process model has been fitted to the CONTROL results and 95% confidence limits have been generated. Clearly, some 3- to 4-yr variations in the CONTROL, presumably ENSO-related, exceed the 95% confidence level and are unlikely to be explained by the integration of white noise forcing. At longer periods the AR1 model provides a better fit, with the CONTROL remaining inside the 95% limits. The extra forcing in the NAT500 simulation leads to it being outside the AR1 95% confidence limits of CONTROL for a wide range of frequencies. A consequence of the increase in natural variability when natural external forcings are included is that it will be more difficult to detect an anthropogenic signal above the background of the natural changes.

3) EFFECT OF VOLCANIC ERUPTIONS

An interesting aspect of the natural externally forced variability, seen as a clear difference in character be-
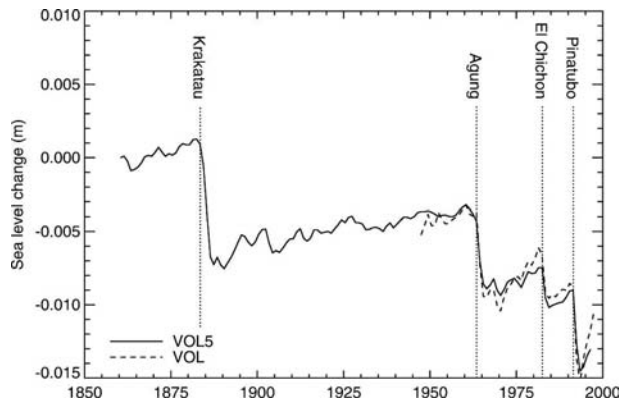
FIG. 5. Annual time series of global-mean sea level change due to thermal expansion in HadCM3 integrations with volcanic forcing only. VOL5 is shifted vertically to start from zero in 1860 and divided by five. VOL is shifted vertically to have the same mean as VOL5 for 1947–96. The vertical dotted lines indicate the years in which particularly large eruptions occurred.

tween the time series of NAT500 and CONTROL (Fig. 3), is the occurrence of large and sudden falls in sea level. These falls coincide with volcanic eruptions, which cause negative radiative forcing for a small number of years. After the Tambora eruption of 1815, the largest in the 500 yr of the simulations, the forcing was strongly negative for three years, reaching approximately -4.75 W m^{-2} (Tett et al. 2006, their Fig. 2), and sea level in NAT500 fell by ~25 mm. Each such fall is followed by an initially rapid rise, but in some cases this is partial, and gradual recovery appears to continue over several decades. A marked fall in sea level could result equally from a large cooling over a thin layer of ocean or a smaller cooling over a thicker layer. However, the slow recovery is consistent only with the latter. If intermediate and deep layers are cooled, the anomaly will persist for longer, because interior heat transport processes are relatively slow. The penetration of the cooling into these layers might be assisted because cooling the surface promotes vertical instability and mixing.

Church et al. (2005) have analyzed the thermal expansion signal of volcanoes using the Department of Energy (DOE) Parallel Climate Model (PCM) AOGCM, by comparing corresponding ensembles of integrations starting in 1890, one ensemble having natural and anthropogenic forcings, the other omitting volcanic forcing. They find a fall of 6 mm following the Pinatubo eruption of 1991; our experiments VOL and VOL5 give the same results (Fig. 5). Church et al. note that the recovery of sea level after an eruption typically takes a decade or more.

Gleckler et al. (2006) have compared ocean heat content changes in six AOGCMs integrated from 1850 or

1860 using anthropogenic and natural forcings with six that had only anthropogenic forcing. They report that the eruption of Krakatau in 1883 caused a substantial ocean cooling that persists for many decades in the deep layers in all the models. The time scale of recovery is model dependent, but there is still a remnant signal at the end of the twentieth century. From comparison of simulations done with anthropogenic and natural forcings separately using the Geophysical Fluid Dynamics Laboratory (GFDL) Climate Model version 2 (CM2) AOGCM, Delworth et al. (2005) similarly conclude that volcanoes in the late nineteenth and early twentieth centuries cause a sudden drop in subsurface ocean temperature from which recovery is slow.

We find the same in VOL5 (Fig. 5). The eruption of Krakatau causes a sea level fall due to thermal expansion, only about half of which has been recovered by the time of the eruption of Agung in 1963. Given the long time scale of recovery from volcanic eruptions, it seems likely that the signal of Tambora must have persisted beyond the end of the nineteenth century. However the time series of NAT500 in Fig. 3 seems to suggest a recovery by about 1850. This is probably because of an increase in solar output that occurred coincidentally (Tett et al. 2006, their Fig. 2).

In VOL5 the volcanic forcing was multiplied by 5, but the response might not scale linearly. Stott et al. (2003) found that it does for global-mean surface air temperature, but this involves mainly the upper ocean. To check the scaling for thermal expansion, we compare with the VOL ensemble mean (Fig. 5, in which VOL5 is divided by 5). Linearity appears to be reasonably satisfied over the short period on which we can compare them, though there is a tendency to recover more quickly from the unmagnified forcing. This could be because the cooling does not penetrate so deeply.

The time series of Fig. 5 suggest the idea that sea level would continue to fall in steps indefinitely when the system is subjected to episodic negative forcing. This could not really be the case, of course. If the sequence of volcanoes is continued, a statistically steady state must be reached eventually. Since the volcanic forcing appears to cool the deep ocean and thus strengthen the vertical temperature gradient, the steady state could be achieved (a) by increasing downward vertical heat transport (through wind-driven and thermohaline overturning and diapycnal mixing) until it balances the average volcanic cooling (b) by decreasing effectiveness of volcanic cooling because the increasing vertical stability will inhibit heat loss from the intermediate layers (for instance through convection). The steady state might be different from the one that results from a constant forcing with the same time average,
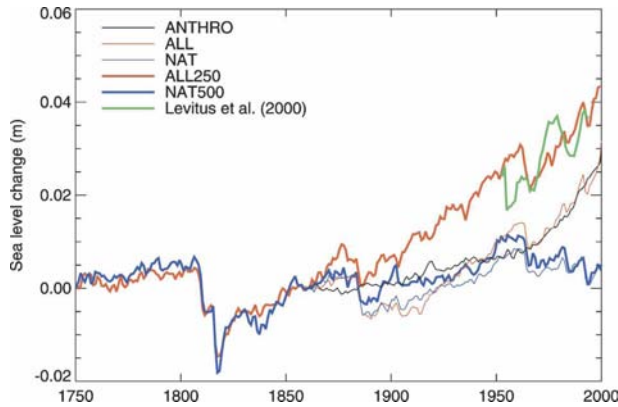
FIG. 6. Annual time series of global-mean sea level change due to thermal expansion from HadCM3 experiments and estimated from the dataset of Levitus et al. (2000) for recent decades. The simulated time series have been shifted vertically so that they all have zero at 1860.

such as is used in the HadCM3 CONTROL, which had been spun up for 1000 yr with average twentieth-century volcanic forcing before the start of NAT500. In that case it would be necessary to spin up the model with episodic negative forcing to obtain a realistic CONTROL steady state. This issue merits further investigation.

4) COMPARISON WITH OBSERVED CHANGES IN RECENT DECADES

On the basis of observed ocean temperatures, Antonov et al. (2005) calculate a thermal expansion contribution to sea level of 0.40 ± 0.05 mm yr^{-1} during 1957–96. For the same period ALL250 gives 0.35 mm yr^{-1}, about 20% smaller. In Fig. 6 we show a comparison with thermal expansion computed by ourselves from the dataset of Levitus et al. (2000), which is an earlier version than that of Antonov et al. (2005) and gives 0.46 ± 0.05 mm yr^{-1}.

As remarked by Antonov et al. (2005), the precise choice of period can make a substantial difference to the observational trend, because of the large multidecadal variability in the observational time series. Despite the inclusion of natural forcing, ALL250 appears to have less variability. A similar difference between model and observation has been discussed previously for the closely related issue of ocean heat content changes (Gregory et al. 2004). It appears that HadCM3 (and other AOGCMs) may not generate enough internal variability. The methods for infilling sparse observational data could also account for some of the discrepancy (Gregory et al. 2004; AchutaRao et al. 2006). We return to this point in section 5d.

Antonov et al. (2005) calculate a rate of 1.23 mm yr^{-1} of thermal expansion during 1993–2003 from the upper 700 m of the ocean, Willis et al. (2004) 1.6 ± 0.3 mm yr^{-1} for the upper 750 m, and Carton et al. (2005) 2.3 ± 0.8 mm yr^{-1} during 1993–2001 for the complete depth. ALL250 gives 1.6 mm yr^{-1} during 1993–2000, in good agreement with the observational estimates.

b. Glaciers

Changes in glaciers and ice caps (i.e., all land ice excluding the ice sheets of Greenland and Antarctica) are more important on century time scales than changes in the ice sheets because they are found in generally warmer and wetter climates, so they experience greater melting and precipitation, and have a greater mass balance sensitivity to temperature change (Oerlemans and Fortuin 1992). In the following, we refer to all of them as "glaciers" for convenience but note that more than half of the total mass is accounted for by the far less numerous ice caps (Meier and Bahr 1996; Raper and Braithwaite 2005).

1) GLACIER MASS BALANCE

The specific mass balance of a glacier is its rate of change of volume divided by its surface area. It is conventionally expressed in meters per year of liquid water equivalent and is zero if the glacier is in balance with its climate. The mass balance sensitivity to temperature b (m yr^{-1} K^{-1}) is defined as the change in specific mass balance per unit rise in temperature and is negative because raising the temperature tends to reduce the mass.

Since only a few dozen of the world's >100 000 glaciers have been studied in sufficient detail to determine their mass balance accurately, characteristic mass balance sensitivities are estimated for larger regions that experience similar climate and climate change. Zuo and Oerlemans (1997) present an inventory of 100 glaciated regions, with areas A_i and sensitivities b_i. The contribution dh/dt of glaciers to the rate of sea level rise is obtained by summing over all regions (index i) and dividing by the surface area A_o of the World Ocean:

$$\frac{dh}{dt} = -\frac{1}{A_o} \sum_i b_i A_i \Delta T_i, \tag{1}$$

where ΔT_i is the temperature difference with respect to a climate in which the glaciers of region i are in a steady state. The effect of changes in precipitation over the glaciers is ignored. Although this can be locally significant, causing advance of glaciers in Scandinavia in recent decades, for example, detailed energy balance

modeling of glaciers suggests that precipitation changes are generally much less important than temperature changes (Raper et al. 2000; Van de Wal and Wild 2001; Oerlemans 2005; Greene 2005).

There are two reasons why we cannot apply Eq. (1) directly to obtain changes in sea level due to glaciers. First, on account of the step in forcing at the start of NAT500, there are long-term drifts in ΔT_i not caused by the subsequent forcing. We would like to make a global correction for this, as we did with thermal expansion, since the data available are not sufficient to evaluate the local drifts accurately. Therefore we need to determine the sensitivity of glacier mass balance to global-mean temperature change [section 4b(2)]. Second, we cannot assume that $\Delta T_i = 0$ in the CONTROL, which is an arbitrarily chosen steady-state climate that does not correspond to any real historical time, so there is no reason why it should give a steady state of glacier mass balance. This difficulty is a basic limitation of our treatment of glacier mass balance and is discussed further in appendix A. We show below [section 4b(3)] how we choose the zero to optimize the match with observed glacier changes.

2) GLOBAL GLACIER MASS BALANCE SENSITIVITY

It is a common result of climate change simulations with AOGCMs that the geographical patterns of annual- or seasonal-mean temperature change are relatively stable while their amplitude evolves with global climate change (e.g., Huntingford and Cox 2000). Hence we can write $\Delta T_i = R_i \Delta T - \theta_i$, where ΔT is the global-mean surface air temperature (SAT) change with respect to the CONTROL climate, R_i is the ratio of temperature change in region i to ΔT, and θ_i is the temperature difference in the CONTROL from the (unknown) steady state for the glaciers in region i. Substituting this form for ΔT_i into Eq. (1), we get

$$\frac{dh}{dt} = b_g(\Delta T - \theta) \quad b_g \equiv -\frac{1}{A_o}\sum_i b_i A_i R_i, \quad (2)$$

where b_g is the global glacier mass balance sensitivity to global-mean temperature change, expressed as sea level equivalent (b_g is positive), and θ is a constant. We evaluate b_g by regressing dh/dt computed from Eq. (1) for NAT500 and ALL250 against ΔT calculated from the same runs (Fig. 7). CONTROL is subtracted from NAT500 in parallel in both calculations to remove the CONTROL drift. Data before 1600 are excluded, since the adjustment to the additional step in radiative forcing is largest in the first century of NAT500 (Fig. 1), and might have a different geographical pattern of temperature change from forced climate change.
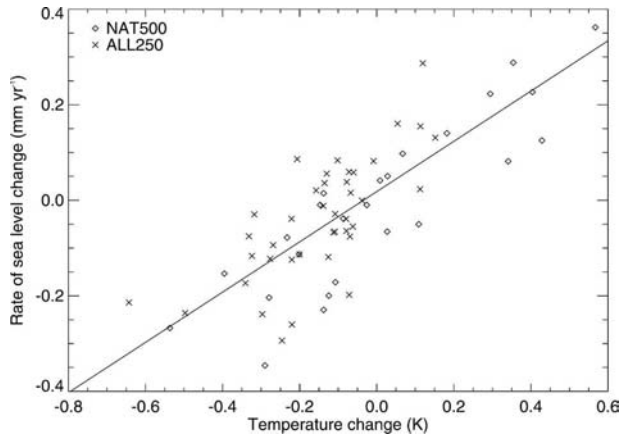

FIG. 7. Decadal means of the glacier contribution to the rate of global-mean sea level rise in NAT500 and ALL250 plotted against global-mean SAT anomaly from CONTROL.

The regression gives $b_g = 0.53 \pm 0.05$ mm yr^{-1} K^{-1}, with a reasonable correlation of 0.80, confirming our assumption that the patterns R_i of temperature change are fairly stable, even though the nature of the forcing is changing in ALL250 from natural to predominantly anthropogenic. Examining individual 50-yr periods for ALL250 shows substantial scatter in b_g but no trend. There is some suggestion that b_g is larger when fitted over shorter periods, perhaps indicating differences in the patterns of temperature change for forcings varying over longer time scales. That might explain why the value of b_g is smaller than diagnosed from HadCM3 for future climate change, for example, $b_g = 0.62$ mm yr^{-1} K^{-1} for scenario IS92a (Church et al. 2001), during which climate changes much more rapidly than in the past.

Using b_g, we can obtain dh/dt from the global ΔT time series, rather than from the latitude–longitude fields. This allows us first to apply a correction for the initial step in forcing, by adjusting ΔT as described in section 2 (Fig. 1), in addition to subtracting the CONTROL drift as before. Then we can compute $h(t)$ as the time integral of dh/dt from Eq. (2). The results have systematic uncertainties of ~10% from the regression and another ~15% from the underlying glacier scheme (Gregory and Oerlemans 1998), making 20% upon combination in quadrature.

3) GLACIER STEADY STATE

The constant θ in Eq. (2) is unknown because of our ignorance of the climate that would give a steady state for global glacier mass. Different θ will result in time series of dh/dt having the same variability but offset by constant amounts. Zuo and Oerlemans (1997) ad-

TABLE 2. Rate of sea level rise dh/dt due to glacier mass change evaluated for various choices of θ, the global-mean SAT difference between the climate in which glacier mass is in balance, and the climate of 1865–94. The value chosen for the simulations was $\theta = -0.05$ K, whose entry is set bold.

θ (K)	Year of minimum h	dh/dt (mm yr^{-1})		
		1900–2000	1961–76	1988–98
0.10	1895	0.14	0.07	0.31
0.05	1895	0.17	0.09	0.33
0.00	1895	0.20	0.12	0.36
−0.05	**1846**	**0.22**	**0.15**	**0.39**
−0.10	1729	0.25	0.17	0.41
−0.15	start	0.28	0.20	0.44
−0.20	start	0.30	0.23	0.47
−0.25	start	0.33	0.25	0.49
−0.30	start	0.36	0.28	0.52

dressed the same issue when modeling global glacier mass balance changes since 1865. On the basis of numerical studies of particular glaciers, they chose $\theta = -0.15$ K for their 1865–94 baseline climate (in which $\Delta T = 0$ by definition), meaning that the baseline global climate was 0.15 K warmer than the glacier steady state, so global glacier mass was being lost during the baseline period and adding to sea level.

We evaluated dh/dt using ΔT from ALL250 for various choices of θ (Table 2), defining θ with respect to the climate of 1865–94 for consistency with Zuo and Oerlemans. To constrain the value of θ, we compared the results with two observations: 1) Around the end of the nineteenth century, glaciers globally attained their maximum extent since the last glacial period. For instance, the stacked glacier time series of Oerlemans (2005) show an increase in length until about 1750 and a retreat since about 1850. We therefore require a minimum in h during this interval. 2) Glacier mass loss contributed about 0.15 mm yr^{-1} to sea level rise during 1961–76 and 0.41 mm yr^{-1} during 1988–98 (Dyurgerov 2003). These estimates are based on a compilation of available mass balance observations, extrapolated to the global scale by area weighting. A revised assessment by Dyurgerov and Meier (2005) gives 0.28 and 0.58 mm yr^{-1} for these periods but generally has larger estimates than independent analyses by Ohmura (2004) and Cogley (2005).

With more positive values of θ, glacier mass generally increases until the late nineteenth century, because the climate is colder than the assumed steady state, and mass is lost during the twentieth century. With more negative values, glaciers lose mass throughout ALL250 since the climate is always warmer than the assumed steady state. Intermediate values give growth before the eighteenth century and contraction during the

twentieth, with maxima around 1720 and 1850 (minima in h). We therefore chose $\theta = -0.05$ K, which is within this intermediate range and gives better overall agreement than $\theta = -0.10$ K for the recent periods. Greater precision in θ cannot be justified, because of the observational uncertainty in glacier mass balance and the internal variability of the climate system. The decadal standard deviation of dh/dt is 0.06 mm yr^{-1} in the CONTROL, implying that the real world and a perfect model of it (two independent realizations with the same anthropogenic and natural forcings) would differ randomly for any given decade with a standard deviation of 0.08 mm yr^{-1}, whereas the difference in dh/dt for 1988–98 for $\theta = -0.05$ K and -0.10 K is only 0.02 mm yr^{-1}. However, an uncertainty of 0.05 K in θ translates into only a small uncertainty of 2.7 mm in sea level when integrated over 100 yr.

c. Ice sheets

Although the continental ice sheets cover many GCM grid boxes, adequate simulation of their mass balance requires a higher resolution than HadCM3, because the majority of precipitation and ablation occur on the steep margins, which are too narrow to be well represented by the GCM topography (Gregory and Lowe 2000). Huybrechts et al. (2004) used results for temperature and precipitation change from short integrations (a decade or two) of high-resolution atmosphere GCMs. They scaled these high-resolution patterns to match the area-average changes over the ice sheets simulated for the twenty-first century under scenario IS92a by various AOGCMs, including HadCM3, and then calculated future mass balance changes for Greenland and Antarctica by applying the scaled high-resolution fields to an ice sheet model at a resolution of 20 km.

Church et al. (2001) found that the mass balance results of Huybrechts et al. (2004) could be reasonably well represented for each ice sheet by a mass balance sensitivity to global temperature change, in the same way that b_g represents global glacier mass balance change. Unlike b_g, the mass balance results for the ice sheets include changes in precipitation as well as in melting. Precipitation change is relatively more important for ice sheets since melting is limited in cold climates. From the HadCM3 results the Greenland sensitivity is $b_G = +0.09 \pm 0.04$ mm yr^{-1} K^{-1} and the Antarctic $b_A = -0.35 \pm 0.05$ mm yr^{-1} K^{-1} (Church et al. 2001, their Table 11.3 and appendix). The latter is negative since there is no melting at all in Antarctica; this number reflects the increase in precipitation (snowfall) expected in a globally warmer climate and assumes that

the rate of dynamic discharge of ice from land (the source of icebergs) does not respond to climate change on the time scales of relevance (cf. e.g., Huybrechts et al. 2004; Alley et al. 2005, for discussion). There is more snowfall in Greenland too, but the increase in melting is greater, so $b_G > 0$. Data from Greenland ice cores characterizing Holocene climate variability have been interpreted as casting doubt on whether AOGCMs are realistic in their prediction of increases in precipitation accompanying warming. We examine this issue briefly in appendix B with HadCM3 and conclude that the model and the data are consistent because the nature of the forcing is different in the two cases.

Comparing $b_G + b_A \simeq -0.24 \pm 0.06$ mm yr^{-1} K^{-1} to the glacier $b_g = 0.53 \pm 0.05$ mm yr^{-1} K^{-1} indicates that the ice sheets would offset about half the glacier contribution. However, there are no comparable observations of historical changes in the ice sheets against which to verify the sensitivities. For the 1990s there are estimates of ice sheet mass changes from airborne and satellite laser altimetry (e.g., Rignot and Thomas 2002; Davis et al. 2005), which translate into sea level contributions of between 0.1 and 0.2 mm yr^{-1} for Greenland and between -0.1 and 0.1 mm yr^{-1} for Antarctica. Since the ice sheets have time scales of millennia for dynamical adjustment, their present mass balance could be affected not only by recent but also by earlier climate change, in particular the termination of the last glacial period. Modeling work reported by Church et al. (2001) suggests that the latter could give a persistent sea level contribution throughout the last 500 yr of between -0.1 and 0.0 mm yr^{-1} from Greenland and between 0.1 to 0.5 mm yr^{-1} from Antarctica, not related to climate change during the period.

Because their contribution is less certain than those of thermal expansion and glaciers but relatively small, we omit the ice sheets from our calculation of global-mean sea level change.

d. Terrestrial water storage

Water could be added to the ocean by reduction of storage on land other than in land ice. Two possibilities are soil moisture and seasonal snow cover. Both of these can be estimated from HadCM3, and we that find they give negligible contributions during the twentieth century, of much less than 0.1 mm yr^{-1} each.

5. Global-mean sea level rise

We calculate the thermal expansion (Fig. 6) and glacier (Fig. 8) contributions to sea level using the methods of sections 4a and 4b for the climate change experiments ALL250, NAT500, ALL, NAT, and ANTHRO
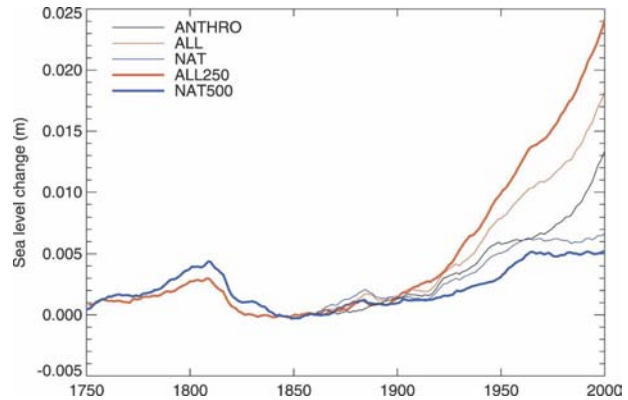

FIG. 8. Annual time series from HadCM3 experiments of global-mean sea level change due to glacier mass loss. The simulated time series have been shifted vertically so that they all have zero at 1860.

(section 2 and Table 1). We add the contributions to obtain our estimate of global-mean sea level rise (Fig. 9). In our simulations, thermal expansion is more important than glaciers for both trend and variability. During the twentieth century, ALL250 indicates that thermal expansion contributed 0.32 mm yr^{-1} to global-mean sea level rise and glaciers 0.22 mm yr^{-1}, the latter being similar to the estimate of Zuo and Oerlemans (1997).

a. Rate of recent sea level rise

The twentieth-century rate of sea level rise (the sum of thermal expansion and glaciers) in ALL250 is 0.54 ± 0.01 mm yr^{-1} (Table 3), considerably less than the rate of 1.0–2.0 mm yr^{-1} estimated from tide gauges by Church et al. (2001) and 1.7 ± 0.3 mm yr^{-1} by Church and White (2006). The analyses of global sea level variations based on tide gauges by Holgate and Wood-
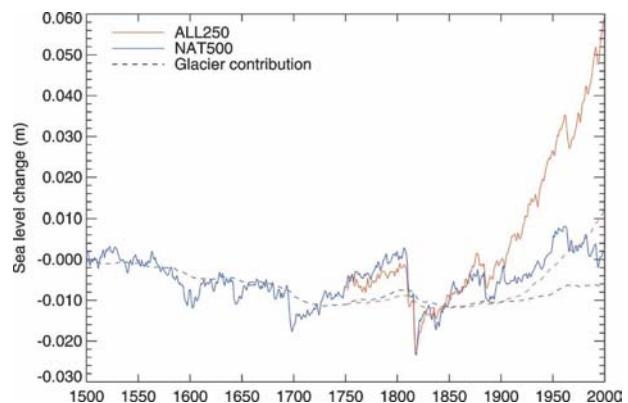

FIG. 9. Annual time series from HadCM3 experiments of global-mean sea level change due to thermal expansion and glacier mass loss.

Table 3. Rates of global-mean sea level rise (linear trends in mm yr^{-1}) for various periods from thermal expansion and glacier mass loss simulated by HadCM3 experiments.

	1870–1900	1900–50	1950–2000	1900–2000	1990–2000	1993–2000
ALL250	-0.05 ± 0.05	0.54 ± 0.02	0.58 ± 0.04	0.54 ± 0.01	1.00 ± 0.28	2.03 ± 0.17
NAT500	-0.15 ± 0.05	0.14 ± 0.01	-0.14 ± 0.02	0.10 ± 0.01	-0.10 ± 0.21	0.66 ± 0.11
ALL	-0.28 ± 0.05	0.44 ± 0.01	0.48 ± 0.03	0.46 ± 0.01	0.90 ± 0.22	1.63 ± 0.08
NAT	-0.34 ± 0.05	0.24 ± 0.01	-0.07 ± 0.02	0.15 ± 0.01	-0.47 ± 0.34	0.81 ± 0.13
ANTHRO	0.12 ± 0.01	0.21 ± 0.25	0.55 ± 0.03	0.32 ± 0.01	1.04 ± 0.02	1.00 ± 0.03

worth (2004) for 1948–2002 and Church et al. (2004) for 1950–2000 give 1.7 ± 0.2 and 1.8 ± 0.3 mm yr^{-1}, while ALL250 has 0.58 ± 0.04 mm yr^{-1}. Such a discrepancy between AOGCMs and observations was also noted by Church et al. (2001) and subsequent authors. As we have seen, the climate-related terms estimated from HadCM3 do agree reasonably well with observational estimates of those terms separately. The explanation of the enigma therefore requires either that both models and observations are substantially in error for at least one of the terms, or that there is a large term that has been omitted from both.

b. Onset of recent sea level rise

Sea level was generally falling in NAT500 during the sixteenth and seventeenth centuries (Fig. 9) because of negative (natural) forcing (Tett et al. 2006, their Fig. 2), as found by Crowley et al. (2003) for ocean heat content. With an increase in solar output (the end of the Maunder Minimum) and a reduced incidence of volcanoes, sea level rose during the eighteenth century but fell again rapidly in the early nineteenth, owing to solar and volcanic forcing, notably the Tambora eruption of 1815. Since it is similar in both NAT500 and ALL250, the recovery during the remainder of the nineteenth century was due principally to natural factors, with anthropogenic forcing beginning to make a difference in the later decades. A qualitative description of the time series of Fig. 9 would be that the modern trend of rising sea level began around 1820, but these experiments suggest this early onset was naturally forced, not anthropogenic. Indeed in the longer context of NAT500 it appears that sea level did not go outside natural variability until the twentieth century.

Sea level rise beginning around 1820 is in agreement with the extrapolation of Church and White (2006) from tide gauge data, slightly earlier than the deduction of Lambeck et al. (2004) from archaeological data that the onset was about 50–150 yr ago, and consistent with the conclusion of Church et al. (2001) from long tide gauge records that the rate of sea level rise was larger in the twentieth century than in the nineteenth. For instance, from the exceptionally long tide gauge record of Stockholm, Sweden, Ekman (1999) found that the rate for 1885–1984 was greater than that for 1774–1884 by 1.01 ± 0.30 mm yr^{-1}, and by comparison with a method of glacial isostatic adjustment he deduced that the rate in the earlier period was indistinguishable from zero. ALL250 agrees in giving 0.00 ± 0.02 mm yr^{-1} for the earlier period, but the difference between the periods is only 0.49 ± 0.02 mm yr^{-1}, because the twentieth-century rate is smaller than observed.

Similar conclusions apply to thermal expansion and glacier changes separately. The majority of the thermal expansion during the nineteenth century was the recovery from Tambora (Fig. 6). The similarity of ALL250 to NAT500 and ALL to NAT in the latter half of the nineteenth century suggests that glacier retreat beginning around 1850 was naturally forced (Fig. 8). Our choice of θ implies that the glacier volume of that time had been built up by earlier climatic cooling (cf. Zuo and Oerlemans 1997). We suggest based on the evidence of NAT500 and ALL250 that the volcanism and solar minimum of the early nineteenth century caused the buildup.

As discussed above (section 3), ALL250 shows a larger warming than ALL during the late nineteenth and early twentieth centuries (Fig. 2). Consequently ALL250 has greater thermal expansion during this period (Fig. 6), and the glacier contribution to sea level rise is ~0.1 mm yr^{-1} larger in ALL250 during the twentieth century (Fig. 8). Thus, the average rate of sea level rise in the twentieth century is greater in ALL250 than in ALL (Table 3). This is probably a response to anthropogenic forcing from emissions before the start of ALL in 1860 (section 3).

c. Acceleration of sea level rise

During the twentieth century the thermal expansion trends in NAT500 and ALL250 are 0.05 and 0.32 mm yr^{-1}, respectively. The contribution from glaciers is also much larger in ALL250 than in NAT500. In the sum, NAT500 gives a rate of sea level rise of 0.15 ± 0.01 mm yr^{-1}, about a quarter of the ALL250 rate of 0.54 ± 0.01

(Table 3). Anthropogenic forcing of sea level rise was therefore dominant during the twentieth century, and responsible for the larger rate during the twentieth than the nineteenth century or any of the previous centuries in the simulation (Fig. 9; cf. Crowley et al. 2003, for ocean heat content).

We would expect increasing anthropogenic forcing during the nineteenth and twentieth centuries to cause a continuous acceleration of the rate of sea level rise. This behavior is evident in earlier climate model simulations (Church et al. 2001; Gregory et al. 2001). However, there is little acceleration in the twentieth-century time series of thermal expansion in ALL250, because of natural forcings. The rate of thermal expansion in NAT500 is positive during the first half of the twentieth century but negative in the second and thus tends to offset the increasing anthropogenic forcing, as noted by Crowley et al. (2003). The same is true for ALL and NAT. Similar compensation shows in the glacier terms, although the natural contribution to the rate is zero rather than negative during the second half of the century. Consequently ALL250 has an acceleration of 0.0020 ± 0.0007 mm yr^{-2} during the twentieth century and ALL 0.0019 ± 0.0006, while ANTHRO has 0.0070 ± 0.0005, more than 3 times larger. While natural forcing has relatively small influence on the average rate, it evidently does affect the acceleration.

This effect could explain why tide gauges do not provide evidence for acceleration *during* the twentieth century (Douglas 1992), though there could be other offsetting factors (Church et al. 2001). Another explanation could be that the tide gauge network is too sparse, so the signal/noise ratio is too low to detect the acceleration (Gregory et al. 2001). Church and White (2006) have reconstructed global sea level fields back to 1870 based on tide gauge records and EOFs from satellite altimetry, using the method of Church et al. (2004), who produced a dataset for 1950–2000. The global mean of the reconstruction should have better signal/noise than individual gauges, and they do indeed detect a significant acceleration of 0.008 ± 0.004 mm yr^{-2} for the twentieth century alone. It is not surprising that the acceleration is larger than in ALL250, since the reconstructed rate is larger.

For 1870–2000, Church and White find a greater acceleration of 0.012 ± 0.003 mm yr^{-2}. Various long individual tide gauge records also yield detectable accelerations of $0.003-0.009$ mm yr^{-2} (Church et al. 2001, and references therein) when the nineteenth century is included. ALL250 agrees qualitatively with these results in having a greater acceleration for 1870–2000 of 0.0047 ± 0.0004 mm yr^{-2} than for 1900–2000. This could happen if the rate of sea level rise increased early
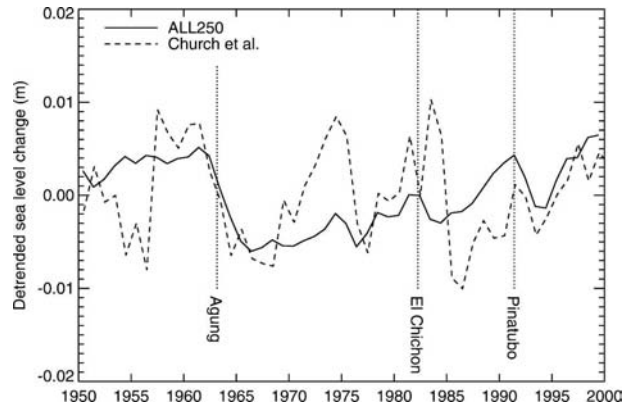

FIG. 10. Time series of annual global-mean sea level change for 1950–2000 from ALL250 and the observationally based dataset of Church et al. (2004), each with its linear trend subtracted.

in the twentieth century. A plausible explanation would be cooling in the late nineteenth century, particularly due to Krakatau, followed by warming in the early twentieth century, particularly due to solar variability (Stott et al. 2000). In support of this, we note that all runs that include natural forcing (i.e., all except ANTHRO) have a negative rate for 1870–1900, and all have a positive rate for 1900–50, even those with natural factors only (NAT500 and NAT; Table 3). Natural factors were thus responsible for the acceleration from the late nineteenth to the twentieth century.

d. Variability of the rate of sea level rise

To assess the variability of the rate of global-mean sea level rise, we compare the time series of ALL250 with the observational dataset of Church et al. (2004; Fig. 10), after detrending both of them, since we have already established that their average rates are markedly different (section 5a). This comparison shows two points.

First, as noted in section 4a(3), drops in sea level following the large volcanic eruptions of Agung (March 1963) and Pinatubo (June 1991) are well simulated; the correspondence is unclear for El Chichon (April 1982). Church et al. (2005) have suggested that rate of global-mean sea level rise for 1993–2003 could have a substantial component due to the recovery from Pinatubo. They estimate from AOGCM results that this could have added 0.5 mm yr^{-1} to the thermal expansion component. The rate of glacier melting would also increase during the recovery of global temperatures. Our results support their idea. Rapid thermal expansion is evident following Pinatubo (Fig. 5). In runs that include natural forcing, the rate of sea level rise for 1993–2000 is much higher than for 1990–2000, by ~1.0 mm yr^{-1} for
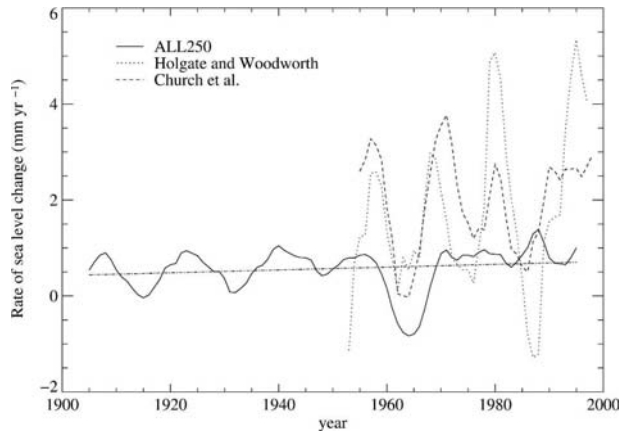
FIG. 11. Time series of rates of global-mean level rise for 10-yr periods from ALL250 and the observationally based datasets of Holgate and Woodworth (2004) and Church et al. (2004). The dotted–dashed line is a least squares fit to the ALL250 time series.
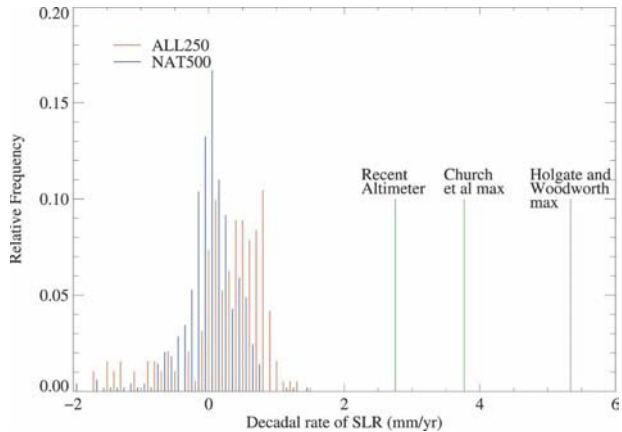

FIG. 12. Histogram of rates of global-mean sea level rise for 10-yr periods since 1800 from NAT500 and ALL250 compared with the rate for 1993–2003 measured by TOPEX/Poseidon (Cazenave and Nerem 2004) and the maximum rates from the datasets of Holgate and Woodworth (2004) and Church et al. (2004).

ALL250, whereas in ANTHRO, the only run not including natural forcing, the rates are practically identical (Table 3).

Second, the observational time series has more variability in general, as found in section 4a(4) for thermal expansion alone. To quantify the variability, we calculated decadal rates of sea level rise for ALL250 by fitting a least squares linear trend to the 10-yr period centered on each year in turn. Rates vary between -0.75 and $+1.5$ mm yr^{-1} over the twentieth century, with both the maximum and the minimum rates occurring after 1950 (Fig. 11). The accelerating trend is small but evident.

We calculated rates for NAT500 and compared them with ALL250 for 1800 onward as a histogram (Fig. 12). The largest negative simulated rates are similar in NAT500 and ALL250 and correspond to the rapid sea level fall following Tambora in 1815, while the largest positive rates occurred during the subsequent recovery. Unsurprisingly, positive rates are much more common in ALL250, especially during the twentieth century; after 1800 the ALL250 rate exceeds the 95th percentile of the NAT500 distribution for 35% of the years.

We calculated decadal rates from the dataset of Church et al. (2004); Holgate and Woodworth (2004) themselves calculated rates from 10-yr running means of the annual data. We compare the time series of rates with ALL250 (Fig. 11). The observational datasets both show significant decadal variability but disagree on its magnitude, with Church et al. having less. This could be because the reconstructed global fields of Church et al. do not attribute as much weight to the variation measured by the tide gauges used by Holgate and Wood-

worth, or because the reconstructed fields contain temporally anticorrelated variability in different regions not sampled by these gauges. Nonetheless, the two time series correlate reasonably well.

The magnitude of the variability in ALL250 is clearly much smaller than in observations, with a standard deviation of 0.5 mm yr^{-1} compared to 1.6 from Holgate and Woodworth and 1.0 from Church et al. for 1955–95 after detrending. We estimate that decadal variability in ice sheet mass balance would add only 0.1 mm yr^{-1} to the standard deviation. The evidence of larger variability than in HadCM3 from the independent observations of ocean temperature and of sea level (from tide gauges), despite its realistic simulation of the response to volcanoes, suggests the conclusion that the model is deficient in decadal internally generated variability. The alternative explanation would be that both kinds of observation contain spurious decadal variability as a result of sparse data.

Since the early 1990s, the TOPEX/Poseidon satellite altimeter has made it possible for the first time to measure sea level rise with near-global coverage. For 1993–2003 the rate of rise was 2.8 mm yr^{-1}, equivalent to 3.1 mm yr^{-1} of ocean (water) volume change after correction for ocean basin volume change associated with glacial isostatic adjustment (Cazenave and Nerem 2004). This rate is substantially more than the average rate for the last half-century (perhaps partly due to recovery from Pinatubo, as noted above). If the entire ALL250 distribution were shifted upward by $\sim$1 mm yr^{-1}, so that its long-term mean matched the observational datasets for the twentieth century, it would barely pro-

duce maximum rates matching the recent decade (Fig. 12). On the other hand, this decade is not exceptional in the datasets of Holgate and Woodworth (2004) and Church et al. (2004; Fig. 11). Again it appears that ALL250 has insufficient decadal variability in the rate of sea level rise.

6. Conclusions

HadCM3 simulations of the last 500 yr with natural and anthropogenic forcings are consistent with evidence from long tide gauges and archaeological data that global-mean sea level began to rise during the first part of the nineteenth century. Anthropogenic greenhouse gas forcing was relatively small at the time; the model results suggest that this apparent early onset was caused by an increase in natural forcing, both from solar variability and as a recovery from the Tambora eruption of 1815. Widespread retreat of glaciers beginning during the nineteenth century is also consistent with this explanation.

The rate of sea level rise was greater during the twentieth century than the nineteenth (or any previous century in the simulation), because greater anthropogenic forcing of climate change (some of it due to emissions during the nineteenth century) led to larger thermal expansion and more rapid glacier retreat. The acceleration of sea level rise *during* the twentieth century was relatively small, that is, the rate was relatively constant, because increasing anthropogenic forcing was partially offset by decreasing natural forcing. Crowley et al. (2003) reached similar conclusions for ocean heat content using a simpler climate model.

The simulated rates of thermal expansion and mass loss by glaciers and ice caps for recent decades are in reasonable agreement with observed estimates of these terms, but their sum ($\sim$0.5 mm yr^{-1}) is less than half of the rate of sea level rise derived from tide gauge records ($\sim$1.8 mm yr^{-1}). Reassessment of glacier mass balance (e.g., Dyurgerov and Meier 2005) might add $\sim$0.2 mm yr^{-1} to their contribution. The model results suggest that it is unlikely that there were large positive contributions from the ice sheets of Greenland and Antarctica or from reductions in seasonal snow cover or soil moisture. On the contrary, the Antarctic ice sheet might have gained mass, offsetting part of the loss of land ice elsewhere. This discrepancy between the sum of the terms and the observed total has been discussed previously by Church et al. (2001), Munk (2002), Woodworth et al. (2004), and other authors.

Recent analyses using ocean in situ salinity measurements (Antonov et al. 2002; Miller and Douglas 2004) have suggested that observed ocean freshening implies that the addition of freshwater to the ocean must have contributed 2–3 times the thermal expansion during the second half of the twentieth century. This would close the gap but is inconsistent with both observations and simulations of land ice changes, and Wadhams and Munk (2004) point out that some of the freshening could be accounted for by net melting of sea ice (not adding mass to the ocean). Another source of water that might be large enough is anthropogenic terrestrial storage, estimated by Church et al. (2001) to lie between -1.1 and $+0.4$ mm yr^{-1} for the twentieth century. The main causes of this are impoundment of water in reservoirs (negative for sea level) and extraction of unreplenished groundwater from aquifers for irrigation, etc. (positive for sea level). Unfortunately the uncertainties are large for these contributions, which have been studied by few authors.

Decadal variability in the rate of thermal expansion in the model is significantly less than calculated from ocean temperature measurements by Antonov et al. (2005). Decadal variability in the simulated rate of sea level rise is significantly less than in the tide gauge reconstructions of Holgate and Woodworth (2004) and Church et al. (2004). Thus, two *independent* types of observational estimate show substantially greater variability than in the simulated ocean. This adds weight to the argument (Levitus et al. 2005) that HadCM3 (and probably other AOGCMs) is deficient in ocean variability. Since there is a reasonable correspondence between simulation and observation in the response to volcanoes, it is likely that the deficiency is in internally generated variability, which is considerably smaller than naturally forced variability in the model. Ocean models of currently typical resolution probably generate very little internal variability, as noted for instance by Gregory et al. (2005). Alternatively it is possible that the observational datasets overestimate the global variability owing to sparse sampling.

Volcanic eruptions cause a sudden fall in sea level and the recovery is slow (Church et al. 2005; Delworth et al. 2005; Gleckler et al. 2006). We suggest that it might be necessary to spin up AOGCMs with episodic negative forcing to produce an average state like that of the real ocean. The large rate of sea level rise ($\sim$3 mm yr^{-1}; Cazenave and Nerem 2004) during the last decade, measured by satellite altimetry, appears from HadCM3 to have had a substantial contribution from the recovery following the Pinatubo eruption of 1991 [as concluded by Church et al. (2005)]. Even so, HadCM3 does not reproduce the observed rate, which however looks less unusual in the context of observed decadal variability (Holgate and Woodworth 2004; Church et al. 2004).

APPENDIX A

Glacier Dynamic Response

The strong influence on the results of the poorly constrained constant θ is a shortcoming of the glacier model. The problem is that Eq. (1) is strictly only a model for perturbations, predicting no steady state except that for $\Delta T_i = 0$. If a raised temperature is maintained, for instance, Eq. (1) suggests that the glaciers will lose mass at a constant rate forever, which is impossible because the glaciers initially have only finite mass. In fact the surface area for melting will be reduced as the volume decreases, restricting the rate of mass loss (Van de Wal and Wild 2001; Church et al. 2001), and this will happen preferentially at lower altitudes. The latter effect in particular means that a new steady state will be reached with a smaller volume and a new distribution of area with altitude. The glaciers will survive in some form unless melting exceeds precipitation even at their highest altitudes.

However, the final steady state and the rate at which it is approached cannot be modeled without glacier dynamics, which determines the evolution of the area altitude distribution. This has been done for individual glaciers (e.g., Oerlemans et al. 1998), but a global treatment requires some statistical or parameterized approach, such as that of Marshall and Clarke (1999) or Raper et al. (2000). A rough idea of the dynamic adjustment can be obtained by assuming that the effect of a temperature perturbation on glacier mass decays exponentially with elapsed time. If the *e*-folding time scale is τ, Eq. (2) becomes

$$\frac{dh}{dt} = b_g \int_0^t \frac{d}{dt} \Delta T(t') \exp[-(t-t')/\tau] dt' +$$
$$b_g [\Delta T(0) - \theta] \exp(-t/\tau), \qquad (A1)$$

where the global temperature is assumed to change from θ (the steady state for glaciers) to $\Delta T(0)$ at time $t = 0$, viewing the subsequent temperature evolution as a sequence of perturbations. For $\tau = \infty$ (i.e., glaciers do not adjust dynamically) we recover Eq. (2). For large enough times the θ term in Eq. (A1) is negligible; the dynamical adjustment means that the initial state is forgotten, and the arbitrary θ disappears. There is no longer a unique steady state, because if ΔT becomes constant at some time, the derivative vanishes in the first term for subsequent times, so as $t \to \infty$ this term decays away, $dh/dt \to 0$ and the glacier volume becomes constant.

Greene (2005) suggests the decay time for Northern Hemisphere glacier volume is about 100 yr. Excursions in ΔT that are completed over decadal time scales will give roughly the same sea level changes from both Eqs. (2) and (A1), but trends over longer periods will produce smaller sea level changes from Eq. (A1) as adjustment is completed to the earlier history. In particular, for ALL250 the glacier contribution to sea level change during the twentieth century is reduced from 22 to 17 mm for $\tau = 100$ yr but becomes insensitive to θ.

APPENDIX B

Relationship between Greenland Temperature and Precipitation

For climate change caused by greenhouse gas forcing, HadCM3 has an increase in precipitation of $5.1 \pm 0.5\%$ K^{-1} for Greenland (temperature change averaged over Greenland, not global ΔT). Precipitation increase generally simulated by AOGCMs (HadCM3 is typical for Greenland; Church et al. 2001) is thermodynamically determined (e.g., Allen and Ingram 2002). Kapsner et al. (1995) show that Greenland ice cores indicate no significant relationship between precipitation and temperature within the Holocene. They argue that the dominant control on precipitation is dynamic through circulation change rather than thermodynamic through temperature change. The ice core evidence might be taken as an argument that the projected precipitation increase is unreliable; if precipitation does not increase over Greenland, the ice sheet will be a larger net contributor to sea level rise in the future (Cuffey and Clow 1997).

An alternative explanation is that the temperature–precipitation relationship is not the same for different kinds of climate variability. In HadCM3 for decadal variations both CONTROL and NAT500 give about 6.5% K^{-1}, but for 100-yr means CONTROL has $8.3 \pm 1.5\%$ K^{-1} while NAT500 has $4.2 \pm 2.5\%$ K^{-1} (the estimate is quite uncertain since NAT500 is only five cen-

turies long). There is a tendency in the model in most parts of Greenland for naturally forced variability to give weaker relationships for longer averaging periods. If instead of using Greenland averages we examine the precipitation–temperature relationship at the single model grid box in which the Greenland summit lies, the site of the Greenland Ice Sheet Project 2 (GISP2) ice cores studied by Kapsner et al., the difference is more marked: the correlation for 100-yr means in NAT500 falls to 0.42 and the slope to $1.3 \pm 1.3\%$ K^{-1}, while they remain higher at 0.82 and $5.9 \pm 0.9\%$ K^{-1} in CONTROL. For 10-yr means under greenhouse gas forcing they are 0.97 and $6.3 \pm 0.3\%$ K^{-1}. The weak relationship in NAT500 is most consistent with the ice core evidence for the Holocene.

The ice cores indicate a temperature–precipitation relationship of 9.5% K^{-1} for the glacial–interglacial transition (Kapsner et al. 1995). In HadCM3 on the Greenland average the difference between the Last Glacial Maximum (LGM) climate (Hewitt et al. 2001) and the preindustrial CONTROL climate gives $4.4 \pm 0.2\%$ K^{-1}. For the GISP2 grid box it is $3.3 \pm 0.4\%$ K^{-1}. However, there is considerable geographical variability, with many Greenland grid boxes showing higher sensitivities. If there is a strong influence of circulation change for the glacial–interglacial transition, as suggested by Kapsner et al. (1995), inaccuracies in the circulation as simulated by HadCM3 in either climate could therefore lead to poor reproduction of the local sensitivity seen in the ice cores.

On the evidence of the HadCM3 runs, we conclude that a marked increase in Greenland precipitation under future anthropogenic climate change is not necessarily inconsistent with the weak or negative precipitation–temperature relationship shown by ice core data from the Holocene (Kapsner et al. 1995; Cuffey and Clow 1997). This is because the forcings have different time scales and causes in the two cases.

REFERENCES

AchutaRao, K. M., B. D. Santer, P. J. Gleckler, K. E. Taylor, D. W. Pierce, T. P. Barnett, and T. M. L. Wigley, 2006: Variability of ocean heat uptake: Reconciling observations and models. *J. Geophys. Res.,* **111,** C05019, doi:10.1029/2005JC003136.

Allen, M. R., and W. J. Ingram, 2002: Constraints on future changes in climate and the hydrologic cycle. *Nature,* **419,** 224–232.

Alley, R. B., P. U. Clark, P. Huybrechts, and I. Joughin, 2005: Ice-sheet and sea-level changes. *Science,* **310,** 456–460.

Antonov, J. I., S. Levitus, and T. P. Boyer, 2002: Steric sea level variations during 1957–1994: Importance of salinity. *J. Geophys. Res.,* **107,** 8013, doi:10.1029/2001JC000964.

——, ——, and ——, 2005: Thermosteric sea level rise, 1955–2003. *Geophys. Res. Lett.,* **32,** L12602, doi:10.1029/2005GL023112.

Carton, J. A., B. S. Giese, and S. A. Grodsky, 2005: Sea level rise and the warming of the oceans in the Simple Ocean Data Assimilation (SODA) ocean reanalysis. *J. Geophys. Res.,* **110,** C09006, doi:10.1029/2004JC002817.

Cazenave, A., and R. S. Nerem, 2004: Present-day sea level change: Observations and causes. *Rev. Geophys.,* **42,** RG3001, doi:10.1029/2003RG000139.

Church, J. A., and N. J. White, 2006: A 20th century acceleration in global sea-level rise. *Geophys. Res. Lett.,* **33,** L01602, doi:10.1029/2005GL024826.

——, J. M. Gregory, P. Huybrechts, M. Kuhn, K. Lambeck, M. T. Nhuan, D. Qin, and P. L. Woodworth, 2001: Changes in sea level. *Climate Change 2001: The Scientific Basis,* J. T. Houghton et al., Eds., Cambridge University Press, 639–693.

——, N. J. White, R. Coleman, K. Lambeck, and J. X. Mitrovica, 2004: Estimates of the regional distribution of sea level rise over the 1950–2000. *J. Climate,* **17,** 2609–2625.

——, ——, and J. M. Arblaster, 2005: Volcanic eruptions: Their impact on sea level and oceanic heat content. *Nature,* **438,** doi:10.1038/nature04237.

Cogley, J. G., 2005: Mass and energy balances of glaciers and ice sheets. *Encyclopedia of Hydrological Sciences,* M. Anderson, Ed., John Wiley, 2555–2573.

Collins, M., S. F. B. Tett, and C. Cooper, 2001: The internal climate variability of HadCM3, a version of the Hadley Centre coupled model without flux adjustments. *Climate Dyn.,* **17,** 61–81.

Crowley, T. J., S. K. Baum, K.-Y. Kim, G. C. Hegerl, and W. T. Hyde, 2003: Modeling ocean heat content changes during the last millennium. *Geophys. Res. Lett.,* **30,** 1932, doi:10.1029/2003GL017801.

Cuffey, K. M., and G. D. Clow, 1997: Temperature, accumulation and ice sheet elevation in central Greenland through the last deglacial transition. *J. Geophys. Res.,* **102,** 26 383–26 396.

Davis, C. H., Y. Li, J. R. McConnell, M. M. Frey, and E. Hanna, 2005: Snowfall-driven growth in East Antarctic ice sheet mitigates recent sea-level rise. *Science,* **308,** doi:10.1126/science.1110662.

Delworth, T. L., V. Ramaswamy, and G. L. Stenchikov, 2005: The impact of aerosols on simulated global ocean temperature and heat content in the 20th century. *Geophys. Res. Lett.,* **32,** L24709, doi:10.1029/2005GL024457.

Douglas, B. C., 1992: Global sea level acceleration. *J. Geophys. Res.,* **97,** 12 699–12 706.

Dyurgerov, M., 2003: Mountain and subpolar glaciers show an increase in sensitivity to climate warming and intensification of the water cycle. *J. Hydrol.,* **282,** 164–176.

——, and M. F. Meier, 2005: Glaciers and changing earth system: A 2004 snapshot. Occasional Note 58, INSTAAR, Boulder, CO, 117 pp.

Ekman, M., 1999: Climate change detected through the world's longest sea level series. *Global Planet. Change,* **21,** 215–224.

Folland, C. K., and Coauthors, 2001: Global temperature change and its uncertainties since 1861. *Geophys. Res. Lett.,* **28,** 2621–2624.

Gleckler, P. J., T. M. L. Wigley, B. D. Santer, J. M. Gregory, K. AchutaRao, and K. E. Taylor, 2006: Volcanoes and climate: Krakatoa's signature persists in the ocean. *Nature,* **439,** doi:10.1038/439675a.

Gordon, C., C. Cooper, C. A. Senior, H. Banks, J. M. Gregory, T. C. Johns, J. F. B. Mitchell, and R. A. Wood, 2000: The simulation of SST, sea ice extents and ocean heat transports in a version of the Hadley Centre coupled model without flux adjustments. *Climate Dyn.,* **16,** 147–168.

Greene, A. M., 2005: A time constant for hemispheric glacier mass balance. *J. Glaciol.,* **51,** 353–362.

Gregory, J. M., and J. Oerlemans, 1998: Simulated future sea-level rise due to glacier melt based on regionally and seasonally resolved temperature changes. *Nature,* **391,** 474–476.

——, and J. A. Lowe, 2000: Predictions of global and regional sea-level rise using AOGCMs with and without flux adjustment. *Geophys. Res. Lett.,* **27,** 3069–3072.

——, and Coauthors, 2001: Comparison of results from several AOGCMs for global and regional sea-level change 1900–2100. *Climate Dyn.,* **18,** 225–240.

——, H. T. Banks, P. A. Stott, J. A. Lowe, and M. D. Palmer, 2004: Simulated and observed decadal variability in ocean heat content. *Geophys. Res. Lett.,* **31,** L15312, doi:10.1029/2004GL020258.

——, and Coauthors, 2005: A model intercomparison of changes in the Atlantic thermohaline circulation in response to increasing atmospheric CO_2 concentration. *Geophys. Res. Lett.,* **32,** L12703, doi:10.1029/2005GL023209.

Hegerl, G. C., T. J. Crowley, S. K. Baum, K. Y. Kim, and W. T. Hyde, 2003: Detection of volcanic, solar and greenhouse gas signals in paleo-reconstructions of Northern Hemispheric temperature. *Geophys. Res. Lett.,* **30,** 1242, doi:10.1029/2002GL016635.

Hewitt, C. D., A. J. Broccoli, J. F. B. Mitchell, and R. J. Stouffer, 2001: A coupled model study of the last glacial maximum: Was part of the North Atlantic relatively warm? *Geophys. Res. Lett.,* **28,** 1571–1574.

Holgate, S. J., and P. L. Woodworth, 2004: Evidence for enhanced coastal sea level rise during the 1990s. *Geophys. Res. Lett.,* **31,** L07305, doi:10.1029/2004GL019626.

Huntingford, C., and P. M. Cox, 2000: An analogue model to derive additional climate change scenarios from existing GCM simulations. *Climate Dyn.,* **16,** 575–586.

Huybrechts, P., J. Gregory, I. Janssens, and M. Wild, 2004: Modelling Antarctic and Greenland volume changes during the 20th and 21st centuries forced by GCM time slice integrations. *Global Planet. Change,* **42,** 83–105.

Kapsner, W. R., R. B. Alley, C. A. Shuman, S. Anandakrishnan, and P. M. Grootes, 1995: Dominant influence of atmospheric circulation on snow accumulation in Greenland over the last 18,000 years. *Nature,* **373,** 52–54.

Lambeck, K., M. Anzidei, F. Antonioli, A. Benini, and A. Esposito, 2004: Sea level in Roman time in the central Mediterranean and implications for recent change. *Earth Planet. Sci. Lett.,* **224,** 563–575.

Levitus, S., J. I. Antonov, T. P. Boyer, and C. Stephens, 2000: Warming of the world ocean. *Science,* **287,** 2225–2229.

——, J. Antonov, and T. Boyer, 2005: Warming of the world ocean, 1955–2003. *Geophys. Res. Lett.,* **32,** L02604, doi:10.1029/2004GL021592.

Marshall, S. J., and G. K. C. Clarke, 1999: Ice sheet inception: Subgrid hypsometric parameterization of mass balance in an ice sheet model. *Climate Dyn.,* **15,** 533–550.

Meier, M. F., and D. B. Bahr, 1996: Counting glaciers: Use of scaling methods to estimate the number and size distribution of the glaciers of the world. *Glaciers, Ice Sheets and Volcanoes: A Tribute to Mark F. Meier,* S. C. Colbeck, Ed., U.S. Army, 89–94.

Miller, L., and B. C. Douglas, 2004: Mass and volume contributions to twentieth-century global sea level rise. *Nature,* **428,** 406–409.

Munk, W., 2002: Twentieth century sea level: An enigma. *Proc. Natl. Acad. Sci. USA,* **99,** 6550–6555.

Oerlemans, J., 2005: Extracting a climate signal from 169 glacier records. *Science,* **308,** 675–677.

——, and J. P. F. Fortuin, 1992: Sensitivity of glaciers and small ice caps to greenhouse warming. *Science,* **258,** 115–117.

——, and Coauthors, 1998: Modelling the response of glaciers to climate warming. *Climate Dyn.,* **14,** 267–274.

Ohmura, A., 2004: Cryosphere during the twentieth century. *The State of the Planet, Geophys. Monogr.,* Vol. 150, Amer. Geophys. Union, 239–257.

Pope, V. D., M. L. Gallani, P. R. Rowntree, and R. A. Stratton, 2000: The impact of new physical parametrizations in the Hadley Centre climate model–HadAM3. *Climate Dyn.,* **16,** 123–146.

Ramaswamy, V., and Coauthors, 2001: Radiative forcing of climate change. *Climate Change 2001: The Scientific Basis,* J. T. Houghton et al., Eds., Cambridge University Press, 349–416.

Raper, S. C. B., and R. J. Braithwaite, 2005: The potential for sea level rise: New estimates from glacier and ice cap area and volume distributions. *Geophys. Res. Lett.,* **32,** L05502, doi:10.1029/2004GL021981.

——, O. Brown, and R. J. Braithwaite, 2000: A geometric glacier model for sea-level change calculations. *J. Glaciol.,* **46,** 357–368.

——, J. M. Gregory, and R. J. Stouffer, 2002: The role of climate sensitivity and ocean heat uptake on AOGCM transient temperature response. *J. Climate,* **15,** 124–130.

Rignot, E., and R. H. Thomas, 2002: Mass balance of polar ice sheets. *Science,* **297,** 1502–1506.

Russell, G. L., V. Gornitz, and J. R. Miller, 2000: Regional sea-level changes projected by the NASA/GISS atmosphere-ocean model. *Climate Dyn.,* **16,** 789–797.

Stott, P. A., S. F. B. Tett, G. S. Jones, M. R. Allen, J. F. B. Mitchell, and G. J. Jenkins, 2000: External control of twentieth century temperature by natural and anthropogenic causes. *Science,* **290,** 2133–2137.

——, G. S. Jones, and J. F. B. Mitchell, 2003: Do models underestimate the solar contribution to recent climate change? *J. Climate,* **16,** 4079–4093.

Tett, S. F. B., and Coauthors, 2002: Estimation of natural and anthropogenic contributions to 20th century temperature change. *J. Geophys. Res.,* **107,** 4306, doi:10.1029/2000JD000028.

——, and Coauthors, 2006: The impact of natural and anthropogenic forcings on climate and hydrology. *Climate Dyn.,* in press.

Van de Wal, R. S. W., and M. Wild, 2001: Modelling the response of glaciers to climate change by applying volume-area scaling in combination with a high resolution GCM. *Climate Dyn.,* **18,** 359–366.

Voss, R., and U. Mikolajewicz, 2001: Long-term climate changes due to increased CO_2 concentration in the coupled atmosphere-ocean general circulation model ECHAM3/LSG. *Climate Dyn.,* **17,** 45–60.

Wadhams, P., and W. Munk, 2004: Ocean freshening, sea level rising, sea ice melting. *Geophys. Res. Lett.,* **31,** L11311, doi:10.1029/2004GL020039.

Willis, J. K., D. Roemmich, and B. Cornuelle, 2004: Interannual variability in upper ocean heat content, temperature, and thermosteric expansion on global scales. *J. Geophys. Res.,* **109,** C12036, doi:10.1029/2003JC002260.

Woodworth, P. L., J. M. Gregory, and R. J. Nicholls, 2004: Long term sea level changes and their impacts. *The Sea,* A. R. Robinson and K. H. Brink, Eds., Harvard University Press, 715–753.

Zuo, Z., and J. Oerlemans, 1997: Contribution of glacier melt to sea level rise since AD 1865: A regionally differentiated calculation. *Climate Dyn.,* **13,** 835–845.